Pergamon

Available online at www.sciencedirect.com
SCIENCE DIRECT

Cement and Concrete Research 34 (2004) 753–758

CEMENT AND CONCRETE RESEARCH

Study on the weathering resistance of fly ash–lime compacts

Shiqun Li*, Jishan Hu, Lui Biao, Xinguo Li

College of Materials Science and Engineering, Jinan University, Jinan, Shandong 250022, People's Republic of China

Received 12 December 2002; accepted 1 April 2003

Abstract

The relationship between the inner quality factors (such as the amount of effective calcium oxide and the pore structure) of steam-cured fly ash–lime compacts (clinker-free) and the environment factors (such as drying shrinkage, freeze–thaw and carbonation, et cetera) have been studied here comprehensively by the simulation weathering examination. Meanwhile, the influences of additives of alkali paste and gypsum on the mechanical properties and pore structure of the compacts have been investigated and discussed, and the effects of interface texture on the mechanical properties have been discussed also. The results suggest that the weathering resistance of the system studied can be improved effectively by means of controlling the fraction of effective calcium oxide (EF_{cao}) and additives, in turn, to improve the interface interlinking. The optimum fraction of EF_{cao} is ~15.3%, alkali paste is about 3.0% and gypsum is 1.7~2.6% (account by SO_3%) if the as-received low calcium-bearing fly ash with low carbon content (<6.0%) has been selected.

Keywords: Fly ash–lime compacts; Weathering resistance; Effective calcium oxide; Additives; Interface texture

1. Introduction

Fly ash, a kind of industrial by-product, has been studied for many years on its behaviors and its applications. Durability, especially the weathering resistance of systems involving fly ash, is of deep concern now in consequence of which many researches have done on this topic [1–5], but most of them just simply focus on an individual process, such as freeze–thaw, carbonation, drying shrinkage, etc. The comprehensive study of durability on the compact fly ash–lime system is rarely reported. In this study, the comprehensive weathering resistance of steam-cured fly ash–lime compacts is clinker-free system. The curing process is performed at about 90 °C under ambient atmosphere. The correlativity of environment factors (freeze–thaw, carbonation and drying shrinkage) with the inner quality factors (EF_{CaO} and pore structure) of this system and the influences of interfaces and additives on the system have been investigated comprehensively by the simulation weathering resistance cycle, which offers experimental basis and theoretical foundation for the production of high-quality steam-cured fly ash–lime products.

2. Experimental

2.1. Raw materials

The chemical compositions of main raw materials have been listed in Table 1.

The main physical properties of raw materials are as the follows:

Fly ash (Class F): bulk volume weight (drying base) is 700~782 g/cm2; fineness is 62.00~66.00% residue of

Table 1
Chemical compositions of main raw materials

Raw materials	L.O.I	SiO_2	Al_2O_3	Fe_2O_3	CaO	MgO	K_2O	N_2O	SO_3
F.A.[a] I	3.64	53.57	32.70	3.08	2.22	1.05			0.24
F.A.[a] II	5.98	49.51	27.18	10.07	4.67	1.23			0.17
Alkali paste	38.62	6.21	2.25	0.93	42.16	2.56	2.37	0.82	
Gypsum	20.8	2.32	1.14	0.21	31.33	0.60			43.43
Lime	Effective CaO: 72.2			CaO: 81.12					

[a] F.A. = fly ash.

* Corresponding author. Tel.: +86-531-276-5853/7027; fax: +86-531-796-3127.
E-mail address: shiqunli@dns.sdibm.edu.cn (S. Li).

0008-8846/$ – see front matter © 2004 Elsevier Ltd. All rights reserved
doi:10.1016/S0008-8846(03)00128-5

Table 2
Proportioning designed for typical specimens (wt.%)

No.	Lime	(EF_{CaO})	F.A.	Sand	Gypsum (SO_3)	Alkali paste (%)	Remark
01	14.0	(13.6)	60.3	20.7	2.0	3.0	F.A. II
02[a]	16.0	(15.3)	59.0	20.7	2.0	3.0	F.A. II
03	18.5	(17.0)	58.0	20.0	2.0	3.0	F.A. II
04	16.0	(15.3)	59.0	20.7	2.0	3.0	F.A. I
05	16.5	(15.8)	61.2	20.7	2.0	0.0	F.A. II

[a] Gypsum fractions of 0.0, 0.65, 1.09, 1.74, 2.61 and 4.34 have still run for sample No. 02.

0.08 mm screen mesh and is 30~32% of 0.15-mm mesh.
Lime: fineness is about 8% residue of 0.08-mm mesh.
Sand: the maximum particle size is 5-mm mesh and the sieve residue is about 21.00% for 1.25-mm mesh and silt-bearing amount is about 2.15 wt.%.

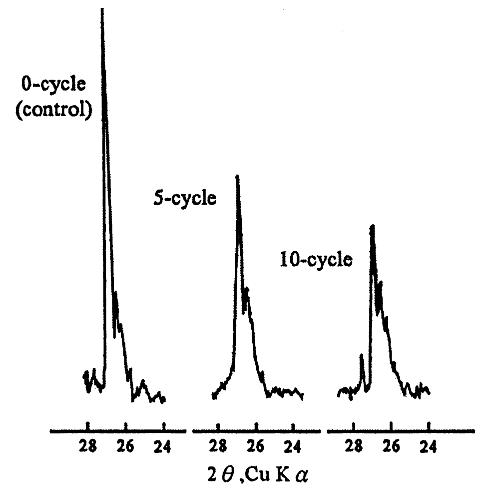

Fig. 2. XRD of typical cycle frequency for specimen No. 02 at $d = 0.334$ m.

2.2. Preparation of compact specimens

The formulations of the compact specimens have been designed as shown in Table 2. The compacts have been moulded in the size of 4×4×12 cm under the pressure of 20 MPa. After demoulding, they are subjected to steam curing at ~90 °C under ambient atmosphere for 7 h. Right after being taken out from the curing chamber, the compacts are subjected to the process of comprehensive weathering resistance cycle that is designed according to the Chinese standard JC239-97. The cycle process is composed by three steps: drying shrinkage, strengthening carbonation (concentration of CO_2 is 90% and the exposure time is 24 h) and freeze and thaw. The compacts in each cycle are exposed 72 h and 15 cycles in all. The properties of strength, carbonation degree, drying shrinkage degree and the mass loss have been examined after each five cycle. The control specimens (without subjected to weathering cycle) have also been performed synchronously.

3. Results and discussions

3.1. Influences of EFCaO on the weathering resistance of compacts

Fig. 1 shows the influences of EF_{CaO} on the strength of specimens before and after weathering cycle (taking the specimens without exposing to weathering cycle as control ones). It can be seen that the compressive strength increases with EF_{CaO} fraction in the range studied here, especially in the range of 13.6 to 15.3%. It can be seen more that the compressive strength increases continuously with the simu-

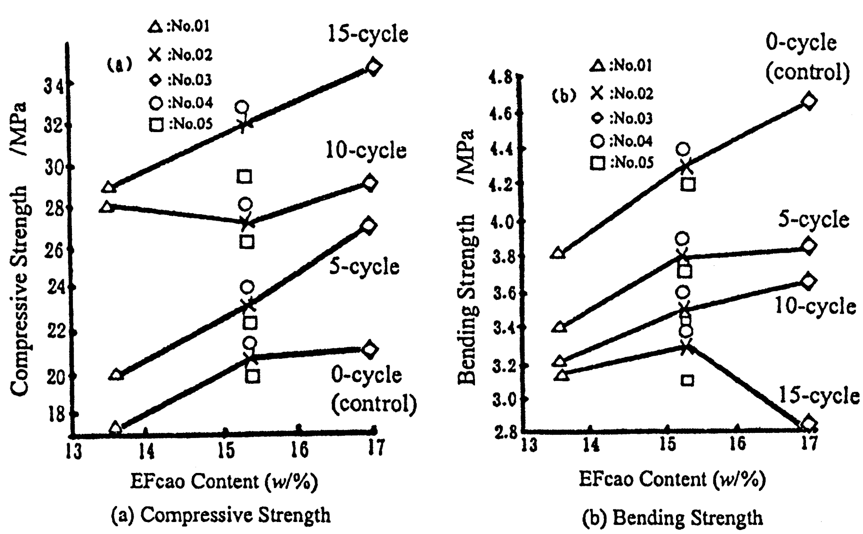

Fig. 1. Strength versus EF_{cao} weight percentage for typical specimens. (a) Compressive strength, (b) bending strength.

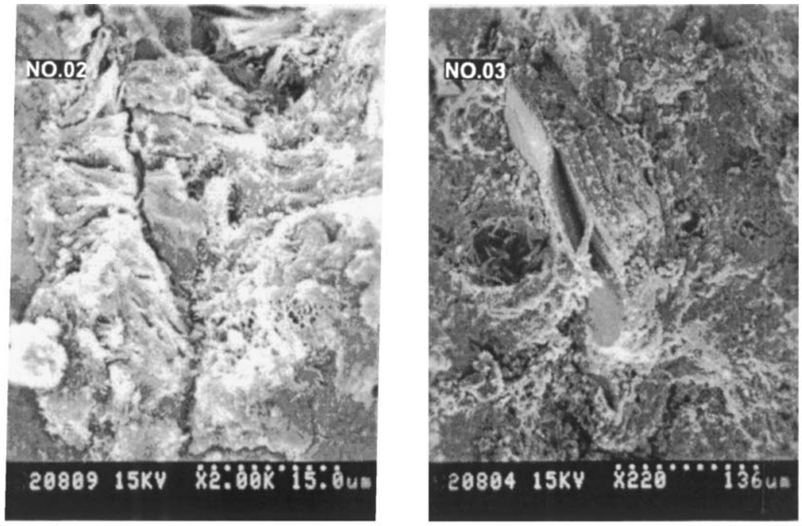

(a) specimen No.02 subjected to 15-cycle, showing the longitudial crack

(b) specimen No.03 showing the grand cystal of $Ca(OH)_2$ when EFcao is high(17.0w/%)

Fig. 3. SEM morphology. (a) Specimen No. 02 subjected to 15 cycles showing the longitudinal crack, (b) specimen No. 03 showing the grand crystal of $Ca(OH)_2$ when EF_{cao} is high (17.0 wt.%).

lation weathering cycle. It may be inferred that this system has a pretty good ability of self-repairing by the continuous hydration and hardening during the process of drying and immersing in water over and over again. XRD in Fig. 2 proves this. The pattern intensity of phase quartz (SiO_2) at the d space of 0.334 nm decreases with cycle frequency. The intensity at d=0.334 nm after 10 cycles decreases about 50% of that for the control compact, and the shape of this pattern becomes wider than that of the control one. It indicates that the network of SiO_2 in F.A. disintegrates markedly under the action of EF_{CaO} (actually effected as well as by the reaction with alkali paste). Moreover, this remarkable disintegrating of SiO_2 network here implies that the significant distortion in the lattice of phase quartz of as-received fly ash occurs, which might be caused by the quick cooling after coal burns at the high temperature in the combustion chamber. And there might also be many unsaturated bonds present in the crystal structure of phase quartz that causes the bonds to break easily at the attack of alkali and earth metal ions. However, the bending strength decreases with the cycle frequency, as shown in Fig. 1b. This may be caused by the existence of longitudinal cracks shown in Fig. 3a; which resulted from the destructive exposures of freeze–thaw and drying shrinkage. Even so, the bending strength of specimens still maintain the range of 3.14 to 3.28 MPa after 15 cycles when EF_{CaO} fraction is in the range of 13.6 to 15.3 wt.%. If EF_{CaO} fraction is too high, such as 17.0%, the bending strength drops markedly at 15 cycles. SEM of Fig. 3b shows that there are some large crystals of $Ca(OH)_2$ in hydration pastes that form the weak bonding at the interface.

Figs. 4 and 5 show the dependence of carbonation and drying shrinkage degree on EF_{CaO} fraction and cycling frequency, respectively, and Table 3. lists the mass loss of specimens after weathering cycles. It presents that the lowest mass loss at the point of EF_{CaO} is 15.3% after 10 cycles. It can be seen that the compacts with proper EF_{CaO} fraction have high weathering resistance by their low degree of carbonation and drying shrinkage and the low mass loss. It is well known that one of the predominant functions of EF_{CaO} here is the excitation of hydration reactivity on fly ash and the hydration reaction mechanism in the system is as follows:

$$CaO + H_2O \rightarrow Ca(OH)_2 \tag{1}$$

$$Ca(OH)_2 + SiO_2 \rightarrow C - S - H \tag{2}$$

$$Ca(OH)_2 + SiO_2 + Al_2O_3 \rightarrow C - S - A - H^{1} \tag{3}$$

The above mechanisms are controlled by the process of solution–deposition in the early stage and by the process of ion diffusing through the reactant layer in the late stage [5,6], and the particle velocity depends upon the solubility of salts in the system. When EF_{CaO} fraction is high, the network structure in fly ash breaks up quickly, and the solubility of soluble salts could be promoted in consequence of which the concentration of ionic groups of $[SiO_4]^{4-}$, $[HAlO_4]^{4-}$, $[H_2AlO_4]^{3-}$, etc., in liquid increases; thereby, the hydration reaction is accelerated in the light of the above Eqs. (1)–(3). Thus, the microstructure of the paste has been improved and the high mechanical and weathering resistant properties of specimens have been present. So it can be known more clearly from Figs. 1–5 and Table 3 that it is not a fact that the more the EF_{CaO} there is, the better the properties are. In other

[1] C, CaO; S, SiO_2; A, Al_2O_3; H, H_2O.

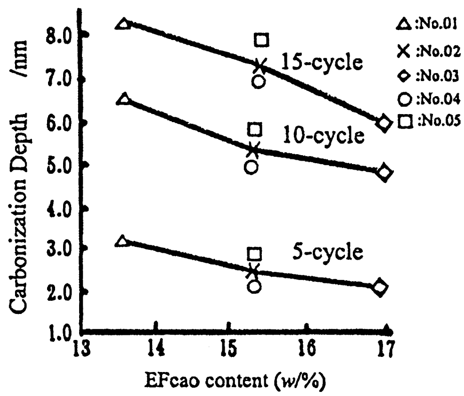

Fig. 4. Carbonization depth versus EF_{cao} content of specimens.

words, EF_{CaO} fraction has to be controlled properly, the optimum fraction of EF_{CaO} here is about 15.3%.

3.2. The influences of additives on the weathering resistance of compacts

3.2.1. Gypsum

It is a controversial topic about whether or not to add gypsum in fly ash steam-curing system among the researchers in this field, such as Yujing and Huisheng [7] and Shiyuan Huang et al. [8]. The results shown in Fig. 6 suggest that appropriate fraction of gypsum is favorable to the strength of specimens, especially to bending strength. SEM in Fig. 7a shows that there are some crystals of $Ca(OH)_2$ that deposit on the surface of fly ash spherical particles together with the hydration product of C-S-H to form an outer shell within the specimens mixing with or without low fraction of gypsum but the texture looks loosely. Fig. 7b shows the fibered or netted texture for the specimen containing 2.0% of SO_3, which might mainly be the hydrated products of C-S-H, C-S-A-H, etc., and the texture is relatively dense. In the compacts with appropriate fraction of gypsum, the ionic groups of $[SiO_4]^{4-}$, $[HAlO_4]^{4-}$, $[H_2AlO_4]^{3-}$, OH^-, etc., might have higher diffusion coefficient than that with low fraction of gypsum; thus, the reaction of $Ca(OH)_2$ with fly ash particles has been promoted, which results in the dense texture and improves the macromechanical property of specimens. In addition, the proper lime slake speed can be obtained before the specimen exposing to steam-curing if an appropriate fraction of gypsum is being provided, which is favorable for reducing the ratio of water to cementitious materials and ensures the materials to maintain sufficient workability during moulding.

Table 3
Mass loss after weather-resistance cycles for typical specimens (wt.%)

No.	EF_{CaO} (%)	Alkali paste (%)	Mass loss (%)	
			10 cycles	15 cycles
01	13.6	3.0	0.066	0.761
02	15.3	3.0	0.017	0.493
03	17.0	3.0	0.079	0.564
04	15.8	3.0		0.652

3.2.2. Alkali paste

Alkali paste, or white paste, is a kind of by-product expelled from a paper plant. It is mainly composed of phase calcium carbonate ($CaCO_3$) and a certain amount of alkali. In comparing specimens No. 02 and 04 with 05 in Figs. 1 and 4, there is no significant difference in strength and in the degree of carbonation at short weathering cycles, but it is not the truth at long cycles. The strength for specimen No. 05 without alkali paste drops sharply after 15 cycles, and the ability of carbonization resistance is weaker than that with alkali paste specimens. It suggests that alkali paste is of advantage for densification of texture—strengthens the ability of freeze–thaw and carbonization for fly ash–lime–water system. In the light of the principle of physicochemistry, the calcium carbonate in alkali paste reacts with $Ca(OH)_2$ and siliceous fly ash in specimens to form complex $nCaCO_3.Ca(OH)_2$ and $CaSiO_3.CaCO_3.Ca(OH)_2.nH_2O$, and to promote the formation of C-S-H in consequence of which the pore structure can be improved. Fig. 8 shows the distribution curve of pore volume versus pore radius of specimens conducted by mercury porosimetry (Quantachrome, USA). Some typical

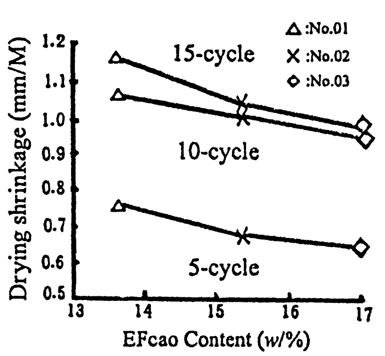

Fig. 5. Values of drying shrinkage versus EF_{cao} of specimens.

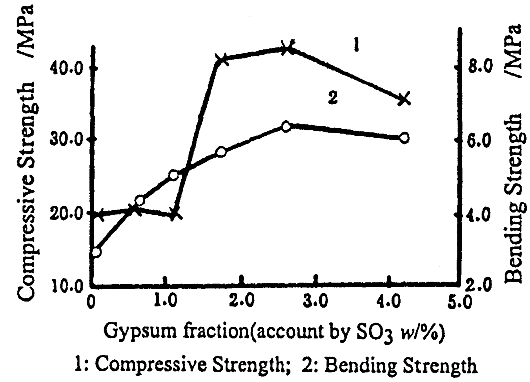

Fig. 6. Influence of gypsum weight fraction on the strength of specimens.

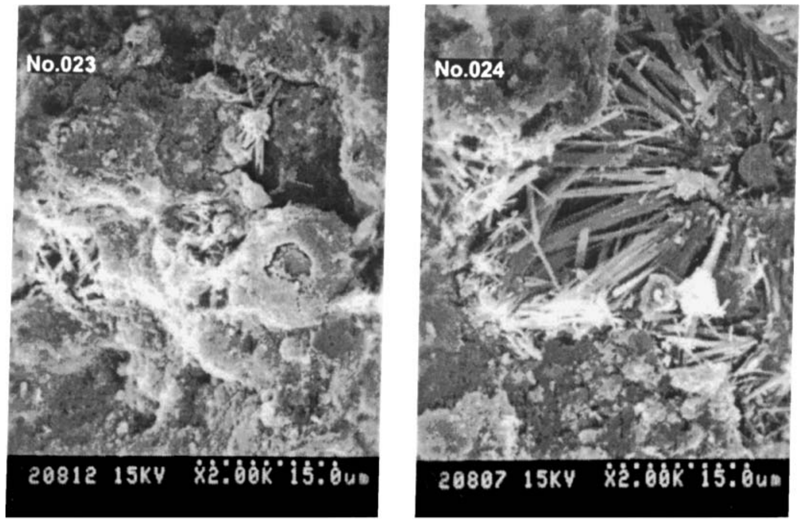

(a) specimen No.02 with 1.09% of SO_3, showing an outer shell around fly ash ball-particale

(b) specimen No.02 with 2.00% of SO_3, showing the fibred or netted nexture

Fig. 7. SEM morphology. (a) Specimen No. 02 with 1.09% of SO_3 showing an outer shell around fly ash ball-particle, (b) specimen No. 02 with 2.00% of SO_3 showing the fibered or netted texture.

pore sizes are listed in Table 4 for specimens No. 02 and 05. It can be seen from them that there is a higher fraction of small pores and lower fraction of large pores in specimen No. 02 than those in No. 05. According to the formula of Kevin, ln P/P_0=2 $M\gamma$/PRT.r, as the pore radius gets small, the corresponding saturated vapor pressure of water or ice in pores goes up, the solubility of ice rises and freezing point decreases; thus, it is not difficult to understand that comprehensive weathering resistance ability of No. 02 is superior to that of No. 05.

3.3. The effects of interface texture on the mechanical properties

The system studied here can be considered as concrete-like one and can be considered as the sands and some inert particles with different sizes in fly ash form as the centroplast and act as a solid frame that confine the shrinkage of specimens, the pores and microcracks filling in with water and air form as negative centroplast. Centroplast is a dispersed part. The hydrates of calcium silicate (C-S-H) in poorly crystalline or gel and hydrocalcium aluminosilicate (C-S-A-H) form as the matrix, which are the continuous part. The hydrated compact here is a heterogeneous system in which only the interface texture between the centroplast and the matrix is in a good interlocking, the mechanical properties of it can be developed. Comparing the SEM morphology of Fig. 3a with b, the transverse cracks occur mainly through the hydration particle in specimen No. 2 with proper formulation, but in specimen with excess EF_{CaO}, the cracks occur along the interface between the large $Ca(OH)_2$ crystal and other hydrates. Here, the large $Ca(OH)_2$ crystal acts as microcentroplast dispersed in the hydration part and brings about the weak interlink interface. When the fraction of EF_{CaO} and gypsum is handled properly, the crystal size of hydrates will be minimized; in turn, the interface linkage will be improved. Again, the morphology of Fig. 7a and b tells the similar situation for the handling of gypsum. As to the negative centroplast, pores and cracks, it is considered as a major factor weakening the strength, but under the attack of carbonation, freeze–thaw and drying shrinkage, the property degradation of specimen depends to a great extent on the pore size and the fraction of pores being filled. On the other hand, it is responsible for the shrinkage of specimens that water is lost only from gel pores of size smaller than 10 nm and from the interlayer of silicate hydration products, and that only the crystalline and struc-

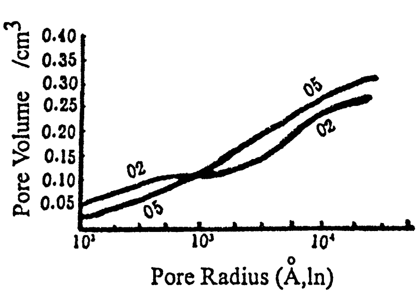

No.02: specimen added with alkali paste;
No.05: specimen added without alkali paste

Fig. 8. Pore distribution curve of typical steam-curing fly ash specimens.

Table 4
Pore size distribution for typical specimens

No.	Porosity (%)	Pore size fraction (%)		
		< 300 Å	100 Å	< 50 Å
02	33.7	45.0	20.0	10.0
05	38.2	26.3	9.6	5.7

tural water get out partially. So the weathering resistance of specimens could be promoted by means of improving the interface linkage. The results shown in Figs. 1, 1, 3, 4, 5 and 8 for specimen Nos. 02 and 05 have indicated that properly handling the factors of EF_{CaO}, alkali paste and gypsum to raise the amount of hydrated calcium silicates and hydrated calcium aluminates, to reduce the amount and size of $Ca(OH)_2$ and to improve the pore distribution; improved interlinking interface can be formed; and finally optimized weathering resistance compacts can be developed.

4. Conclusions

(1) The comprehensive simulation weathering resistance study on the system of fly ash–lime conducted here has revealed the good correlativity of the environment factors (freeze–thaw, carbonation and dry shrinkage) with the inner quality factors (fraction of EFCaO, pore structure and microstructure) and additives.
(2) Appropriately handling the fraction of EFCaO, alkali paste and gypsum can efficiently disintegrate the network of SiO2 in fly ash and improve the hydration reactivity of the system studied.
(3) To improve the pore structure, microstructure and the interface texture, to strengthen the mechanical property and to enhance the weather-resistance ability of specimens, it is necessary to control the appropriate fraction of EF_{CaO}, alkali paste and gypsum. The recommended optimum range of these factors studied here is ~15.3%, 3.0% and 1.7~2.6%, respectively.

References

[1] W. Sun, J. Liu, H. Qin, Y. Zhang, Z. Jin, M. Qian, Fatigue performance and equations of roller compacted concrete with fly ash, Cem. Concr. Res. 28 (2) (1998) 309–316.
[2] W. Zhongwei, L. Huizhen, High Performance Concrete, Chinese Railway Press, Beijing, 1999.
[3] E.P. Kearsley, P.J. Wainwright, The effect of high fly ash content on the compressive strength ff foamed concrete, Cem. Concr. Res. 31 (1) (2001) 105–112.
[4] S. Danshen, Sustainable development of science and technology of fly ash utilization in China, J. Build. Mater. 1 (2) (1998) 170–174 (in Chinese).
[5] Z. Gu, H. Zhen, Carbonization-resistance of lime–fly ash steam-cured, J. Chinese Ceram. Soc. 14 (4) (1986) 478–493 (in Chinese).
[6] C. Wang, Fly ash brick, J. Hunan Build. Mater. (1) (1982) 10–11 (in Chinese).
[7] Z. Yujing, S. Huisheng, Study on composite for base pavement made of waste gypsum from TiO_2 production and fly ash, J. Build. Mater. 3 (4) (2000) 3328–3334 (in Chinese).
[8] H. Shiyuan, L. Zihua, C. Jiping, Reaction kinetics in the system of fly ash-CaO-H_2O, J. Chinese Ceram. Soc. 14 (1) (1986) 191–197 (in Chinese).